第十二届“新物理研讨会”（原威海新物理研讨会）
The 12th Workshop on New Physics (Weihai Workshop on NP)
山东青岛，July 23-29, 2023

Single Transverse Spin Asymmetry as a New Probe of SMEFT Dipole Operators

Xin-Kai Wen (文新锴 Bhung Sing-Kai)

Peking University

In collaboration with Bin Yan, Zhite Yu and C.-P. Yuan

Basing on arXiv: 2307.05236 and works in progress

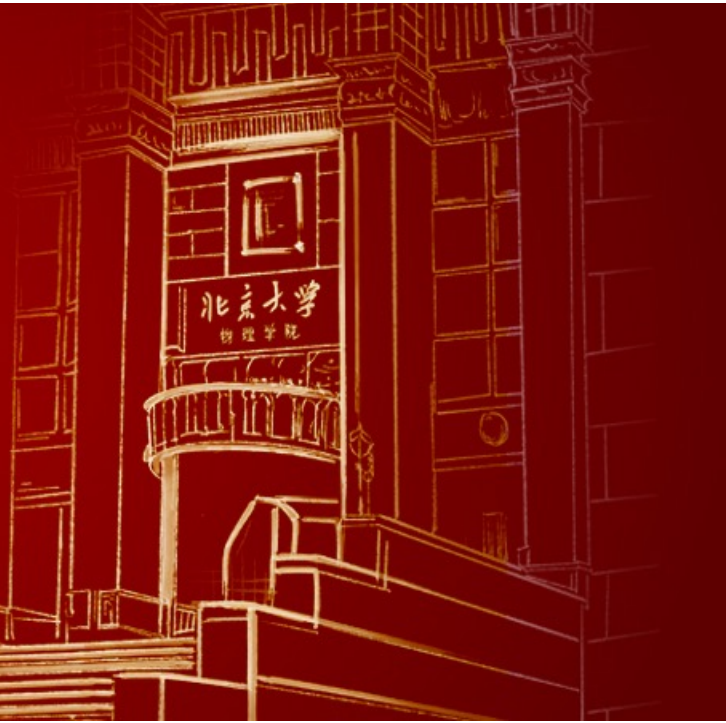

Thanks a lot to the organizers of ITP-CAS and SDU

Qingdao, Shandong, China

2023/07/27

New Physics and SMEFT

None new fundamental resonance since 2012

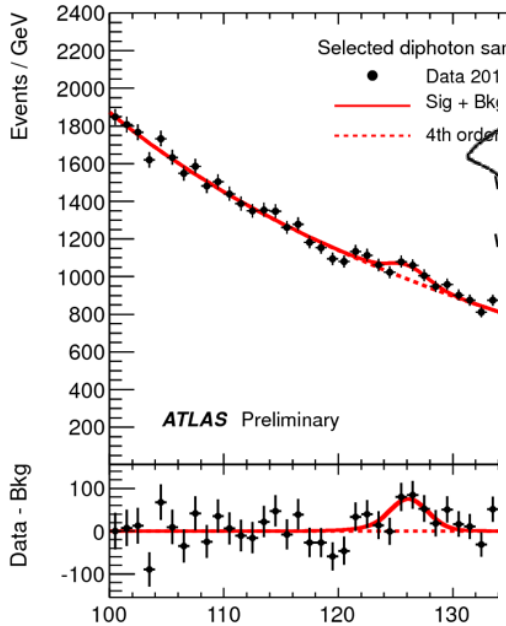

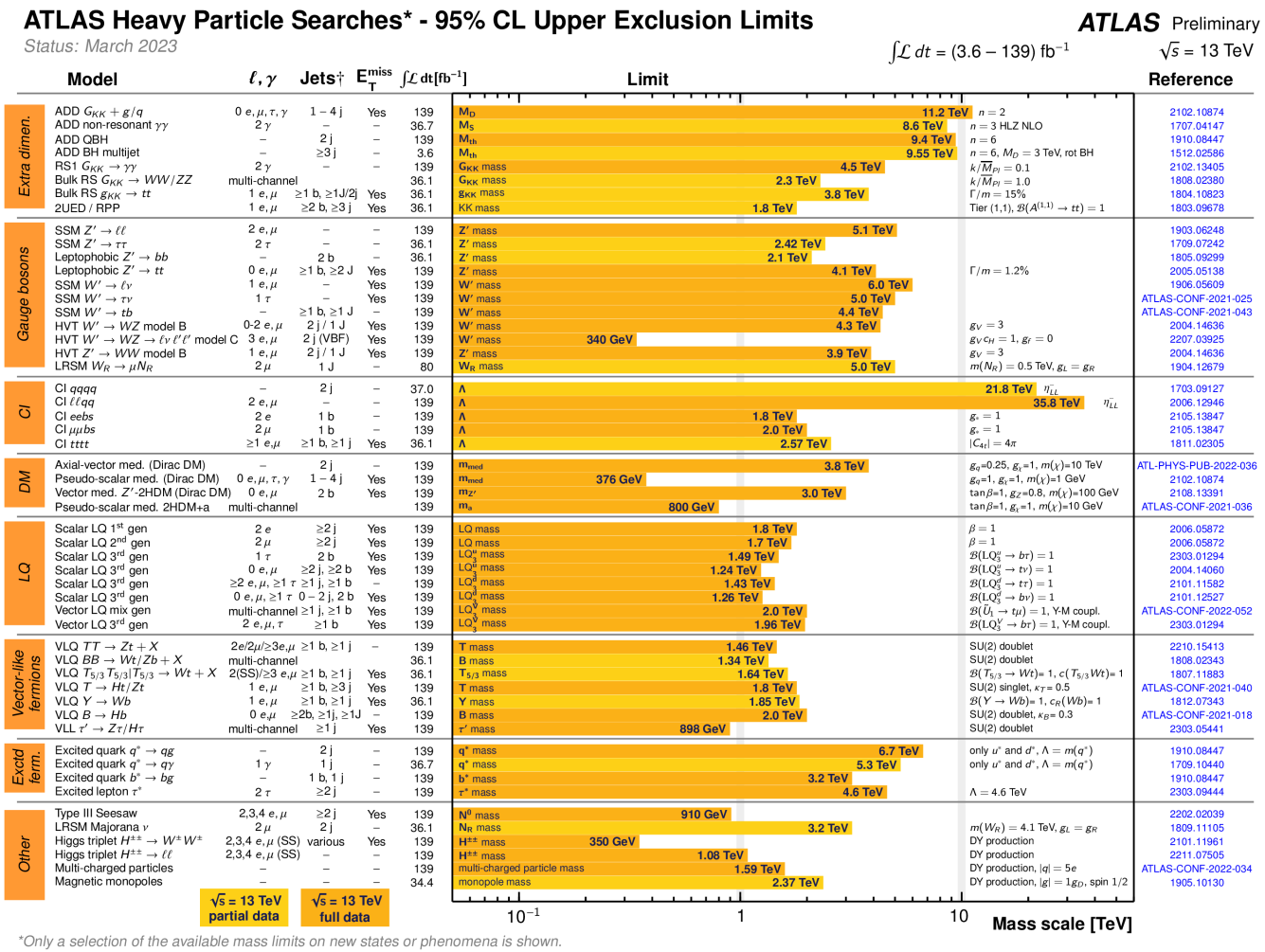

New Physics and SMEFT

None new fundamental resonance since 2012 but anomalies bursting

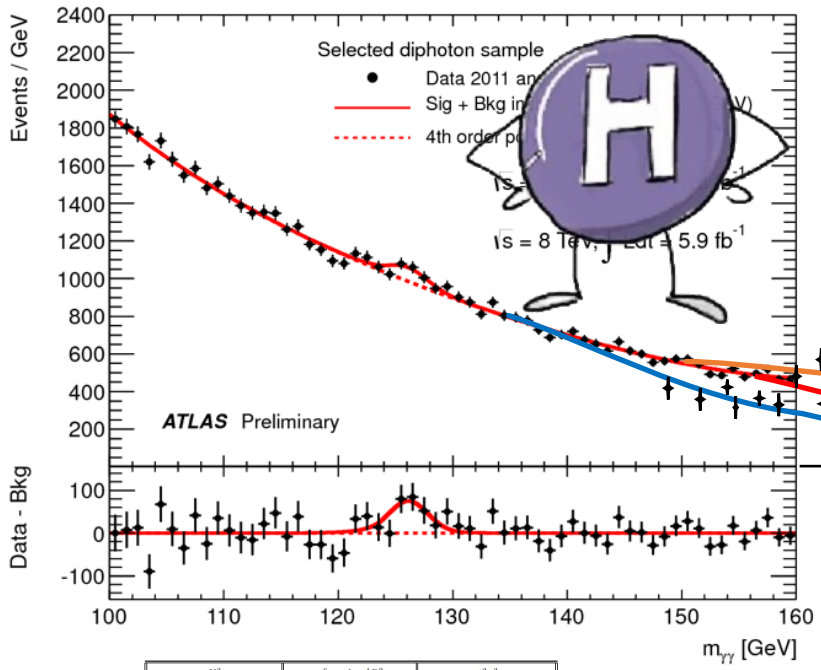

"5W1H": Where, What, Why, When, Who, How ***NP***

NP might hide within the current scale

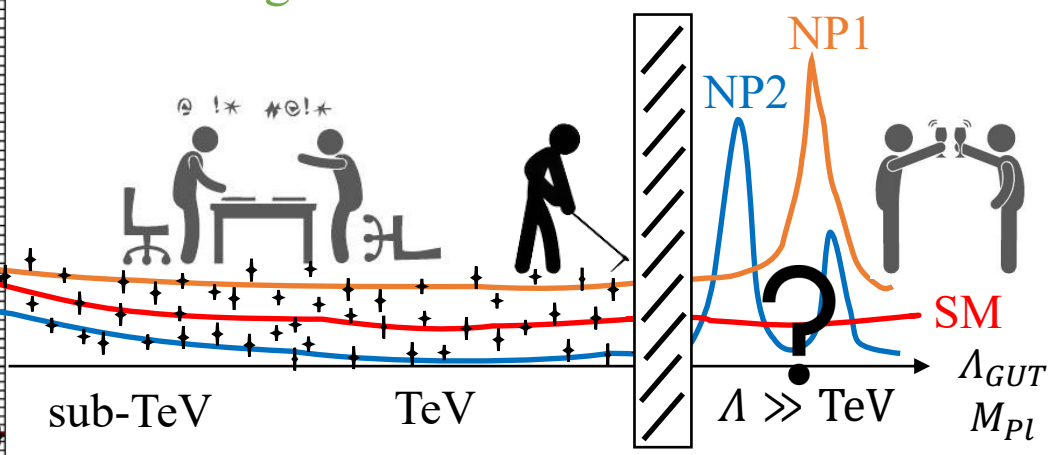

X^3		φ^6 and $\varphi^4 D^2$		$\psi^2\varphi^3$	
Q_G	$f^{ABC} G_\mu^{A\nu} G_\nu^{B\rho} G_\rho^{C\mu}$	Q_φ	$(\varphi^\dagger\varphi)^3$	$Q_{e\varphi}$	$(\varphi^\dagger\varphi)(\bar l_p e_r \varphi)$
$Q_{\widetilde G}$	$f^{ABC} \widetilde G_\mu^{A\nu} G_\nu^{B\rho} G_\rho^{C\mu}$	$Q_{\varphi\Box}$	$(\varphi^\dagger\varphi)\Box(\varphi^\dagger\varphi)$	$Q_{u\varphi}$	$(\varphi^\dagger\varphi)(\bar q_p u_r \widetilde\varphi)$
Q_W	$\varepsilon^{IJK} W_\mu^{I\nu} W_\nu^{J\rho} W_\rho^{K\mu}$	$Q_{\varphi D}$	$\left(\varphi^\dagger D^\mu\varphi\right)^\star \left(\varphi^\dagger D_\mu\varphi\right)$	$Q_{d\varphi}$	$(\varphi^\dagger\varphi)(\bar q_p d_r \varphi)$
$Q_{\widetilde W}$	$\varepsilon^{IJK} \widetilde W_\mu^{I\nu} W_\nu^{J\rho} W_\rho^{K\mu}$				

Q_{eG}	$(\bar l_p \sigma^{\mu\nu} e_r)\tau^I \varphi W_{\mu\nu}^I$	$Q_{\varphi l}^{(1)}$	$(\bar l_p \gamma^\mu l_r)$	$Q_{\varphi l}^{(1)}$	$(\bar l_p \gamma^\mu l_r)$
$Q_{e\widetilde G}$	$(\bar l_p \sigma^{\mu\nu} e_r)\tau^I \widetilde\varphi W_{\mu\nu}^I$	$Q_{\varphi B}$	$(\bar l_p \sigma^{\mu\nu} e_r)\varphi B_{\mu\nu}$	$Q_{\varphi l}^{(3)}$	$(\bar l_p \tau^I \gamma^\mu l_r)$
$Q_{e\varphi W}$	$(\bar l_p e_r \tau^I \varphi) W_\mu^I W^{I\mu}$	Q_{uG}	$(\bar q_p \sigma^{\mu\nu} T^A u_r)\widetilde\varphi\, G_{\mu\nu}^A$	$Q_{\varphi e}$	$(\varphi^\dagger i\overleftrightarrow{D}_\mu \varphi)(\bar e_p \gamma^\mu e_r)$
$Q_{e\varphi\widetilde W}$	$(\bar l_p e_r \tau^I \widetilde\varphi) W_\mu^I W^{I\mu}$	Q_{uW}	$(\bar q_p \sigma^{\mu\nu} u_r)\tau^I \widetilde\varphi\, W_{\mu\nu}^I$	$Q_{\varphi q}^{(1)}$	$(\varphi^\dagger i\overleftrightarrow{D}_\mu \varphi)(\bar q_p \gamma^\mu q_r)$
$Q_{e\varphi B}$	$(\bar l_p e_r \varphi) B_{\mu\nu} B^{\mu\nu}$	Q_{uB}	$(\bar q_p \sigma^{\mu\nu} u_r)\widetilde\varphi\, B_{\mu\nu}$	$Q_{\varphi q}^{(3)}$	$(\varphi^\dagger i\overleftrightarrow{D}_\mu^I \varphi)(\bar q_p \tau^I \gamma^\mu q_r)$
$Q_{e\varphi\widetilde B}$	$(\bar l_p e_r \varphi) \widetilde B_{\mu\nu} B^{\mu\nu}$	Q_{dG}	$(\bar q_p \sigma^{\mu\nu} T^A d_r)\varphi\, G_{\mu\nu}^A$	$Q_{\varphi u}$	$(\varphi^\dagger i\overleftrightarrow{D}_\mu \varphi)(\bar u_p \gamma^\mu u_r)$
Q_{eWB}	$(\bar l_p \tau^I e_r \varphi) W_{\mu\nu}^I B^{\mu\nu}$	Q_{dW}	$(\bar q_p \sigma^{\mu\nu} d_r)\tau^I \varphi\, W_{\mu\nu}^I$	$Q_{\varphi d}$	$(\varphi^\dagger i\overleftrightarrow{D}_\mu \varphi)(\bar d_p \gamma^\mu d_r)$
$Q_{e\widetilde WB}$	$(\bar l_p \tau^I e_r \widetilde\varphi) W_{\mu\nu}^I B^{\mu\nu}$	Q_{dB}	$(\bar q_p \sigma^{\mu\nu} d_r)\varphi\, B_{\mu\nu}$	$Q_{\varphi ud}$	$(\varphi^\dagger i\overleftrightarrow{D}_\mu \varphi)(\bar u_p \gamma^\mu d_r)$

$(\bar LR)(\bar RL)$	
Q_{ledq}	$(\bar l_p^j e_r)(\bar d_s q_t^j)$
$Q_{quqd}^{(1)}$	$(\bar q_p^j u_r)\varepsilon_{jk}(\bar q_s^k d_t)$
$Q_{quqd}^{(8)}$	$(\bar q_p^j T^{\mathrm{A}} u_r)\varepsilon_{jk}(\bar q_s^k T^{\mathrm{A}} d_t)$
$Q_{lequ}^{(1)}$	$(\bar l_p^j e_r)\varepsilon_{jk}(\bar q_s^k u_t)$
$Q_{lequ}^{(3)}$	$(\bar l_p^j \sigma_{\mu\nu} e_r)\varepsilon_{jk}(\bar q_s^k \sigma^{\mu\nu} u_t)$

$(\bar LL)(\bar LL)$	
Q_{ll}	$(\bar l_p \gamma_\mu l_r)(\bar l_s \gamma^\mu l_t)$
$Q_{qq}^{(1)}$	$(\bar q_p \gamma_\mu q_r)(\bar q_s \gamma^\mu q_t)$
$Q_{qq}^{(3)}$	$(\bar q_p \gamma_\mu \tau^I q_r)(\bar q_s \gamma^\mu \tau^I q_t)$
$Q_{lq}^{(1)}$	$(\bar l_p \gamma_\mu l_r)(\bar q_s \gamma^\mu q_t)$
$Q_{lq}^{(3)}$	$(\bar l_p \gamma_\mu \tau^I l_r)(\bar q_s \gamma^\mu \tau^I q_t)$

Table 3: Four-fermion operators.

SMEFT

EWPO

Global Fitting

but some constrained poorly

because of non-interfering effect

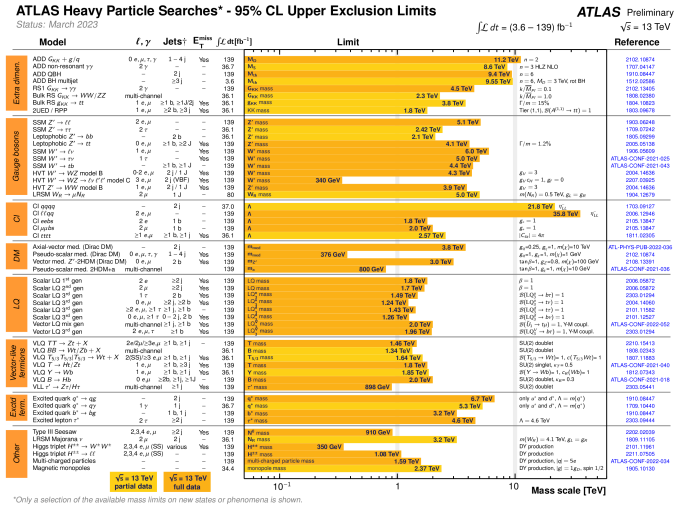

B. Grzadkowski, et al. *JHEP* 10 (2010).

Dipole Operator

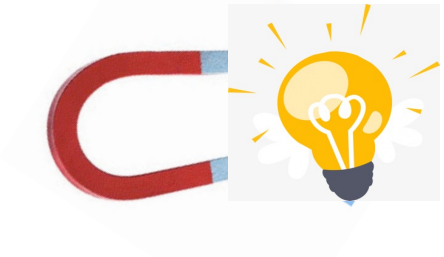

- ✓ Connect Mass and E/M Dipole Moment
- ✓ Loop-induced by the UV BSM
- ✓ Cause Chirality Flip

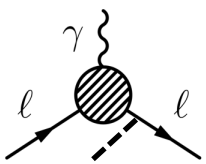

especially for the "4.2$\boldsymbol{\sigma}$"
Direct & Dominant

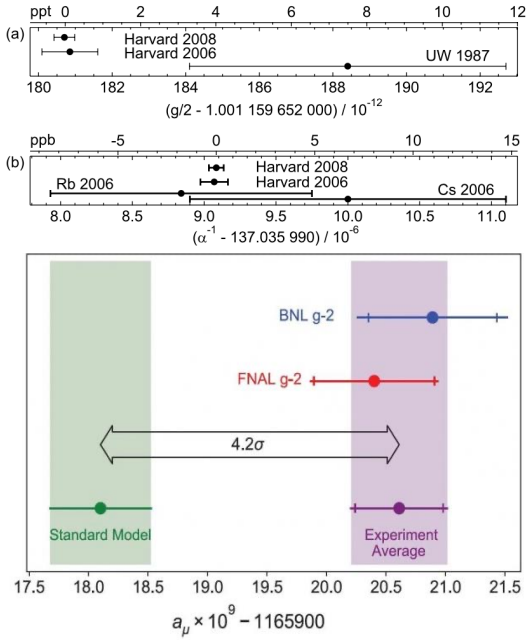

D. Hanneke et al., *Phys.Rev.Lett.* 100,(2008)
G.W. Bennett et al. *Phys.Rept.* 887 (2020)
B. Abi et al. *Phys.Rev.Lett.* 126 (2021)

Loop-induced by the BSM

- Encode information about heavy particle interactions
- Indirect probes of quantum effects of NP

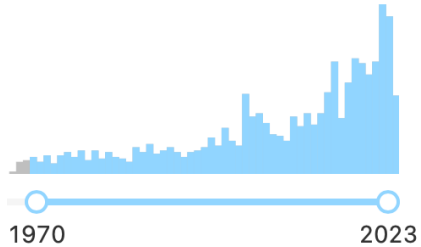

Z' and dark photon model
NMSSM (SUSY)
Scalar extension……

F. Wang et al. *Universe* 9 (2023), 2305.04623
J. Cao et al., 2306.06854
J. Liu et al., *JHEP* 03 (2019), 1810.11028

Chirality flip
Disappear in massless SM

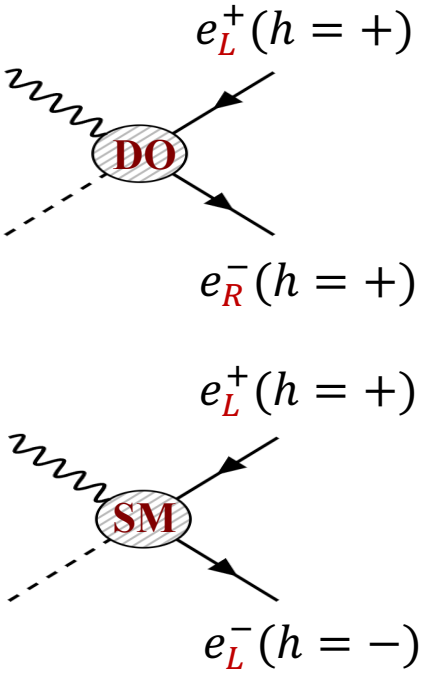

Proposal and Data for Dipole Operator

In Global Analyses, EW dipole couplings constrained poorly

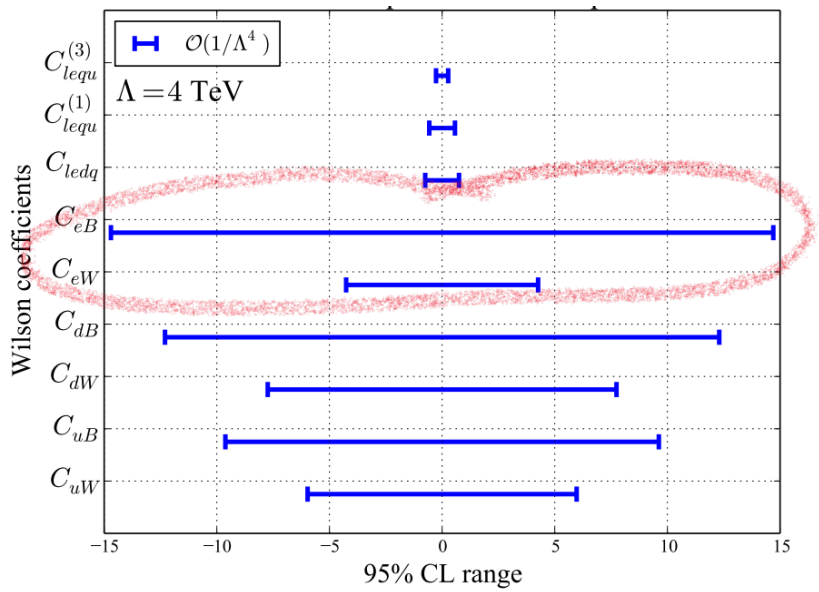

Single-Parameter-Analysis from recent Drell-Yan Data at LHC

(R. Boughezal et al. *Phys.Rev.D* 104 (2021)…)

only small non-interfering effect with $\left|\frac{c_{dipole}}{\Lambda^2}\right|^2$

LHC Drell-Yan: $O(10^{-2}\sim10^{-1})$

(R. Boughezal et al. *Phys.Rev.D* 104 (2021)…) Even if HL-LHC, lifting fifth at most

LEP Z-boson partial width: $O(10^{-2}\sim10^{-1})$

(R. Escribano et al. *Nucl.Phys.B* 429 (1994), S. Schael et al. *Phys.Rept.* 427 (2006)…)

EFT running for interpretation $(g-2)_e$: $O(10^{-6}\sim10^{-2})$

(A. V. Manohar et al. *JHEP* 07 (2021), T. Giani et al. 2302.06660, J. J. Ethier et al. *JHEP* 11 (2021)…)

How to Probe Dipole Operator

Our proposal:

- ✓ C_{dipole}/Λ^2, interfering with the massless SM
- ✓ Without depending on other NP operators
- ✓ Transverse polarization effect
- ✓ Non-trivial azimuthal angular distribution

Single Transverse Spin Azimuthal Asymmetries

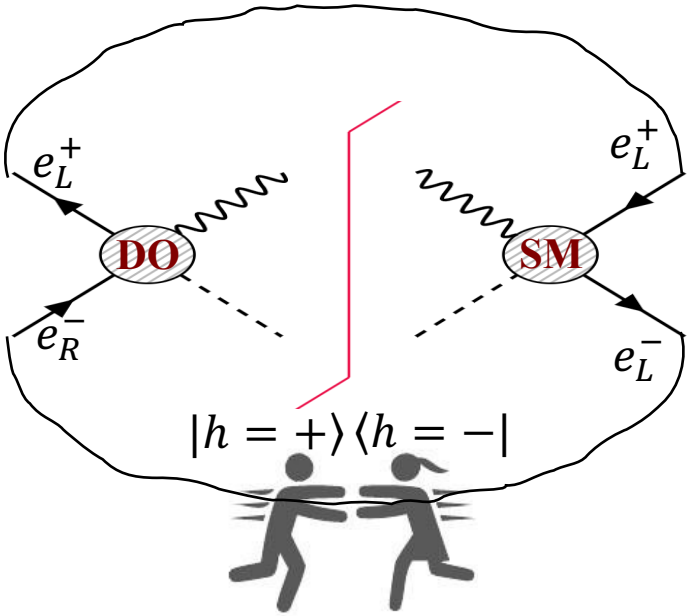

Traditional method via cross section and width

- ➢ $|C_{dipole}|^2/\Lambda^4$, small effect from non-interference
- ➢ Bothered by other operators and assumptions

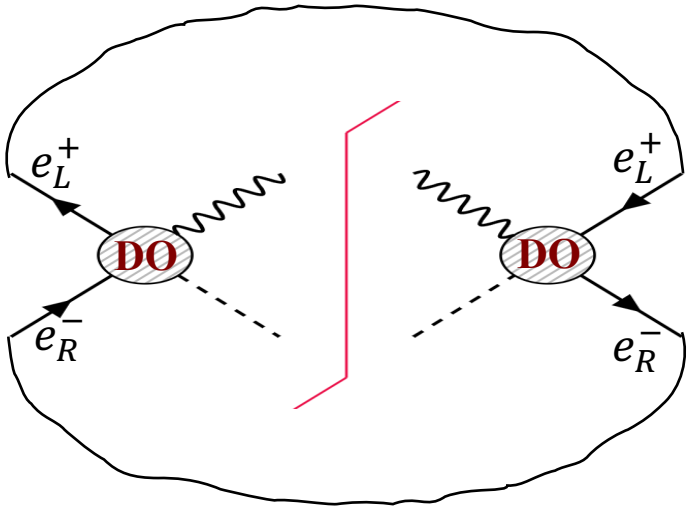

Transverse Spin Polarization

Transverse polarization effect → Interference of helicity amplitudes

Breaking the rotational invariance & A nontrivial azimuthal behavior

Ken-ichi Hikasa, *Phys.Rev.D* 33 (1986) 3203, *PhysRevD.*38 (1988) 1439

$$|\mathcal{M}|^2 = \rho_{\alpha_1\alpha_1'}(\boldsymbol{s})\rho_{\alpha_2\alpha_2'}(\bar{\boldsymbol{s}})\mathcal{M}_{\alpha_1\alpha_2}(\phi)\mathcal{M}^*_{\alpha_1'\alpha_2'}(\phi)$$

$$\boldsymbol{s} = (b_1, b_2, \lambda) = (b_{\rm T}\cos\phi_0, b_{\rm T}\sin\phi_0, \lambda)$$

$$\rho = \frac{1}{2}(1+\boldsymbol{\sigma}\cdot\boldsymbol{s}) = \frac{1}{2}\begin{pmatrix} 1+\lambda & b_{\rm T}e^{-i\phi_0} \\ b_{\rm T}e^{i\phi_0} & 1-\lambda \end{pmatrix}$$

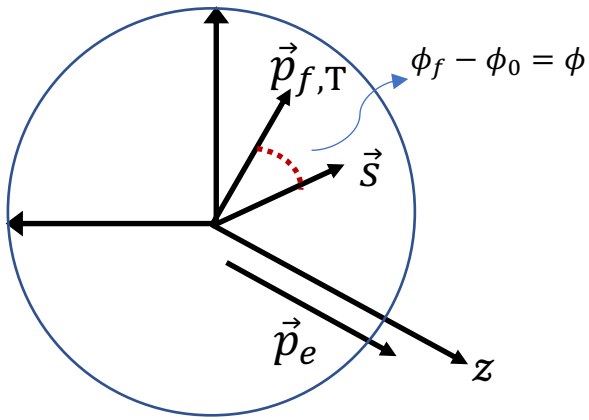

Only the azimuthal difference between initial $\vec{s}$ and finial $\vec{p}_f$ physical meaningful

Only dipole operator contribute to $\mathcal{M}_{\pm\pm}$ while $\mathcal{M}^{\rm SM}_{\pm\pm} = 0$, massless SM only $\mathcal{M}_{\pm\mp} \neq 0$

	U	L	T
U	$\lvert\mathcal{M}\rvert^2_{UU} \to 1$	$\lvert\mathcal{M}\rvert^2_{UL} \to 1$	$\lvert\mathcal{M}\rvert^2_{UT} \to \cos\phi, \sin\phi$
L	$\lvert\mathcal{M}\rvert^2_{LU} \to 1$	$\lvert\mathcal{M}\rvert^2_{LL} \to 1$	$\lvert\mathcal{M}\rvert^2_{LT} \to \cos\phi, \sin\phi$
T	$\lvert\mathcal{M}\rvert^2_{TU} \to \cos\phi, \sin\phi$	$\lvert\mathcal{M}\rvert^2_{TL} \to \cos\phi, \sin\phi$	$\lvert\mathcal{M}\rvert^2_{TT} \to 1, \cos 2\phi, \sin 2\phi$

G. Moortgat-Pick et al. *Phys.Rept.* 460 (2008), *JHEP* 01 (2006)

A New Probe of Dipole Operators

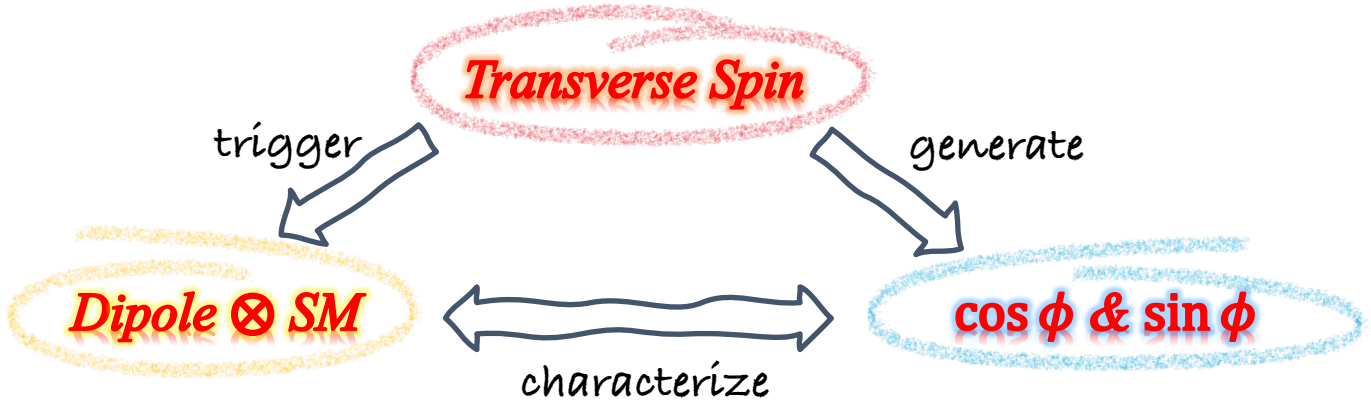

Aligned Spin

$$\phi_0 = \bar{\phi}_0 = 0$$

Opposite Spin

$$(\phi_0, \bar{\phi}_0) = (0, \pi)$$

$$\frac{2\pi\, d\sigma^i}{\sigma^i\, d\phi} = 1 + \underbrace{A_R^i(b_T, \bar{b}_T)}_{\mathrm{Re}[C_{dipole}]} \cos\phi + \underbrace{A_I^i(b_T, \bar{b}_T)}_{\mathrm{Im}[C_{dipole}]} \sin\phi + \underbrace{b_T\, \bar{b}_T\, B^i \cos 2\phi}_{\text{SM \& other NP}} + \mathcal{O}(1/\Lambda^4)$$

$\vec{s} \cdot \vec{p}_f \propto \cos\phi$	$\vec{s} \times \vec{p}_f \propto \sin\phi$	
CP-conserving	CP-violation	

Linearly dependent on the dipole couplings C_{dipole} and spin b_T

Using azimuthal asymmetry instead of polarization asymmetry

$$A_{LR}^i = \frac{\sigma^i(\cos\phi > 0) - \sigma^i(\cos\phi < 0)}{\sigma^i(\cos\phi > 0) + \sigma^i(\cos\phi < 0)} = \frac{2}{\pi} A_R^i$$

$$A_{UD}^i = \frac{\sigma^i(\sin\phi > 0) - \sigma^i(\sin\phi < 0)}{\sigma^i(\sin\phi > 0) + \sigma^i(\sin\phi < 0)} = \frac{2}{\pi} A_I^i,$$

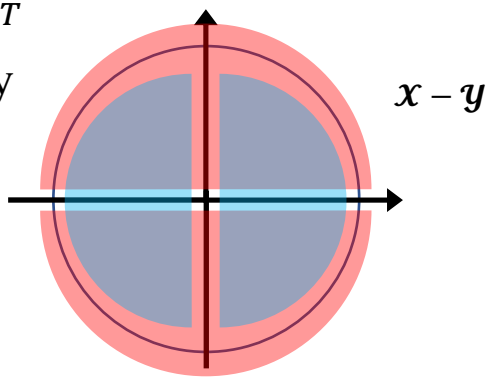

Pinning down Dipole Operators

$$\mathcal{L}_{\text{eff}} = -\frac{1}{\sqrt{2}}\bar{\ell}_L \sigma^{\mu\nu}\left(g_1 \Gamma_B^e B_{\mu\nu} + g_2 \Gamma_W^e \sigma^a W^a_{\mu\nu}\right)\frac{H}{v^2} e_R + \text{h.c.}$$

$$A^i_{LR} = \frac{\sigma^i(\cos\phi > 0) - \sigma^i(\cos\phi < 0)}{\sigma^i(\cos\phi > 0) + \sigma^i(\cos\phi < 0)} = \frac{2}{\pi} A^i_R$$

Aligned Spin

$$\phi_0 = \bar{\phi}_0 = 0$$

Opposite Spin

$$(\phi_0, \bar{\phi}_0) = (0, \pi)$$

$$\sqrt{s} = 250\ \text{GeV}, \mathcal{L} = 5\ \text{ab}^{-1}$$

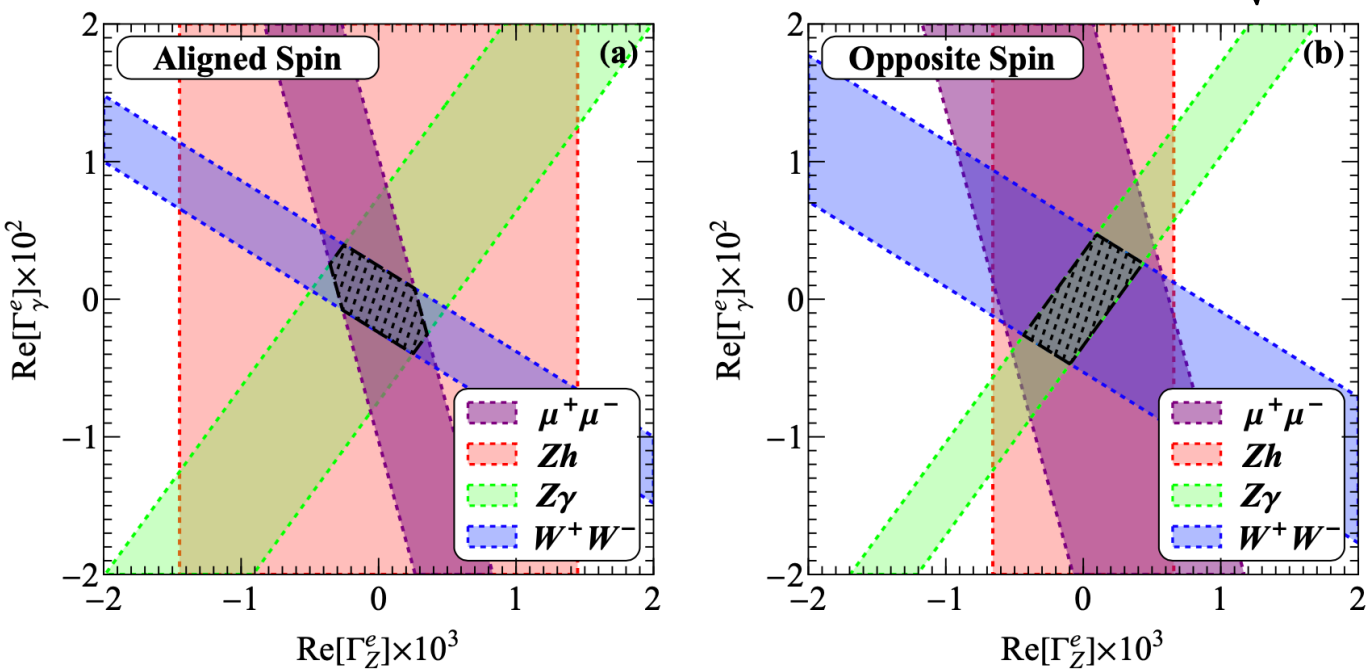

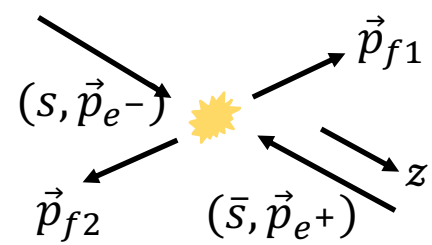

CP property

$$e^+e^- : |e^-(\boldsymbol{s})e^+(\bar{\boldsymbol{s}})\rangle \xrightarrow{\mathcal{CP}} |e^-(\bar{\boldsymbol{s}})e^+(\boldsymbol{s})\rangle \qquad A^i(\boldsymbol{s}_T, \bar{\boldsymbol{s}}_T; \Gamma^e_{Z,\gamma}) = \pm A^i(\bar{\boldsymbol{s}}_T, \boldsymbol{s}_T; \Gamma^{e*}_{Z,\gamma})$$

$$Zh, Z\gamma : |\phi, \theta\rangle \xrightarrow{\mathcal{CP}} |\phi + \pi, \pi - \theta\rangle \qquad (A_R^{WW,\mu\mu}, A_I^{Zh,Z\gamma}) \propto \boldsymbol{s}_T + \bar{\boldsymbol{s}}_T$$

$$W^+W^-, \mu^+\mu^- : |\phi, \theta\rangle \xrightarrow{\mathcal{CP}} |\phi, \theta\rangle \qquad (A_I^{WW,\mu\mu}, A_R^{Zh,Z\gamma}) \propto \boldsymbol{s}_T - \bar{\boldsymbol{s}}_T$$

Pinning down Dipole Operators

$$\mathcal{L}_{\text{eff}} = -\frac{1}{\sqrt{2}}\bar{\ell}_L \sigma^{\mu\nu}\left(g_1 \Gamma_B^e B_{\mu\nu} + g_2 \Gamma_W^e \sigma^a W_{\mu\nu}^a\right)\frac{H}{v^2} e_R + \text{h.c.}$$

$$A_{LR}^i = \frac{\sigma^i(\cos\phi > 0) - \sigma^i(\cos\phi < 0)}{\sigma^i(\cos\phi > 0) + \sigma^i(\cos\phi < 0)} = \frac{2}{\pi} A_R^i$$

Aligned Spin

$$\phi_0 = \bar{\phi}_0 = 0$$

Opposite Spin

$$(\phi_0, \bar{\phi}_0) = (0, \pi)$$

$$\sqrt{s} = 250\ \text{GeV}, \mathcal{L} = 5\ \text{ab}^{-1}$$

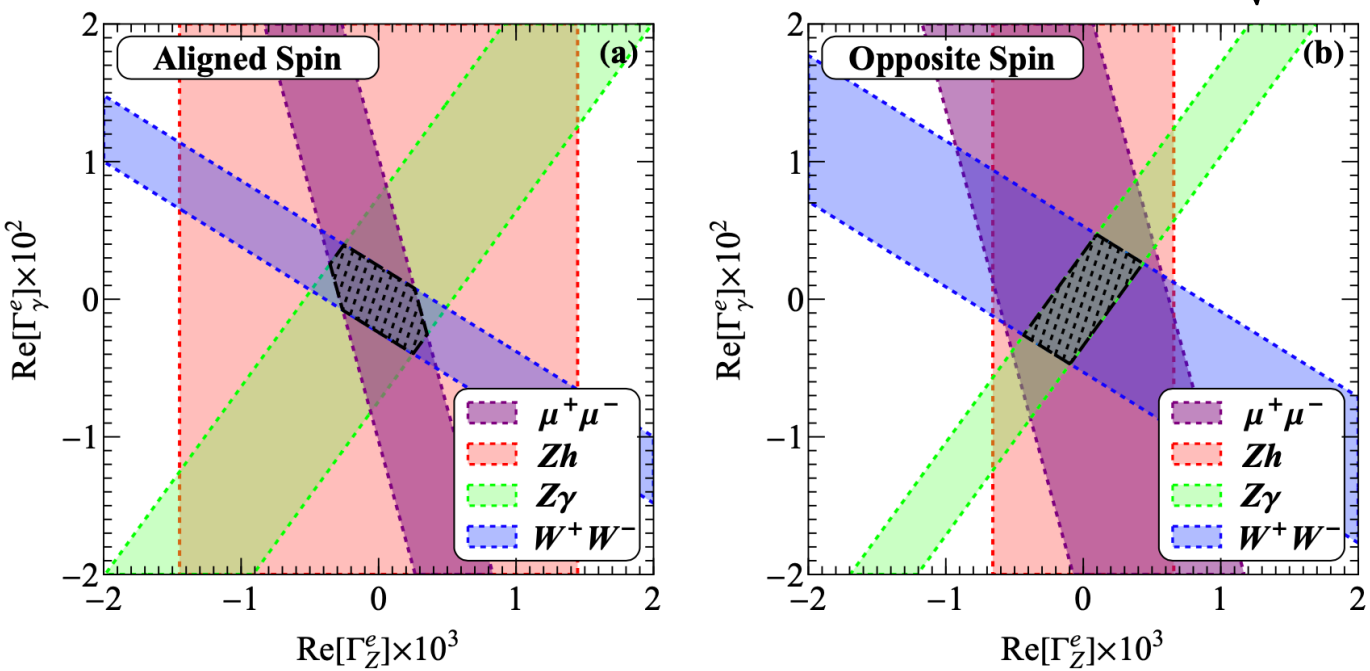

$$A_{R\backslash I}(\Gamma_\gamma^e) < A_{R\backslash I}(\Gamma_Z^e)$$

- SM $(g_L^e + g_R^e) \ll 1$
- SM $WW\gamma < WWZ$
- $\Gamma_W^e = \Gamma_Z^e + s_W^2 \Gamma_\gamma^e$

Parity property

$$\mathcal{M}_{++}^* \mathcal{M}_{-+} = -\mathcal{M}_{+-}^* \mathcal{M}_{--} (g_L \leftrightarrow g_R) \qquad |\mathcal{M}|_{1\phi}^2 \sim (g_L - g_R)[(g_L^e + g_R^e)\Gamma_\gamma^e + \Gamma_Z^e]$$

Pinning down Dipole Operators

For the imaginary parts of dipole couplings, things are similar

Aligned Spin

$$\phi_0 = \bar{\phi}_0 = 0$$

Opposite Spin

$$(\phi_0, \bar{\phi}_0) = (0, \pi)$$

$$A^i_{UD} = \frac{\sigma^i(\sin\phi > 0) - \sigma^i(\sin\phi < 0)}{\sigma^i(\sin\phi > 0) + \sigma^i(\sin\phi < 0)} = \frac{2}{\pi} A^i_I$$

$\sqrt{s} = 250$ GeV, $\mathcal{L} = 5$ ab^{-1}

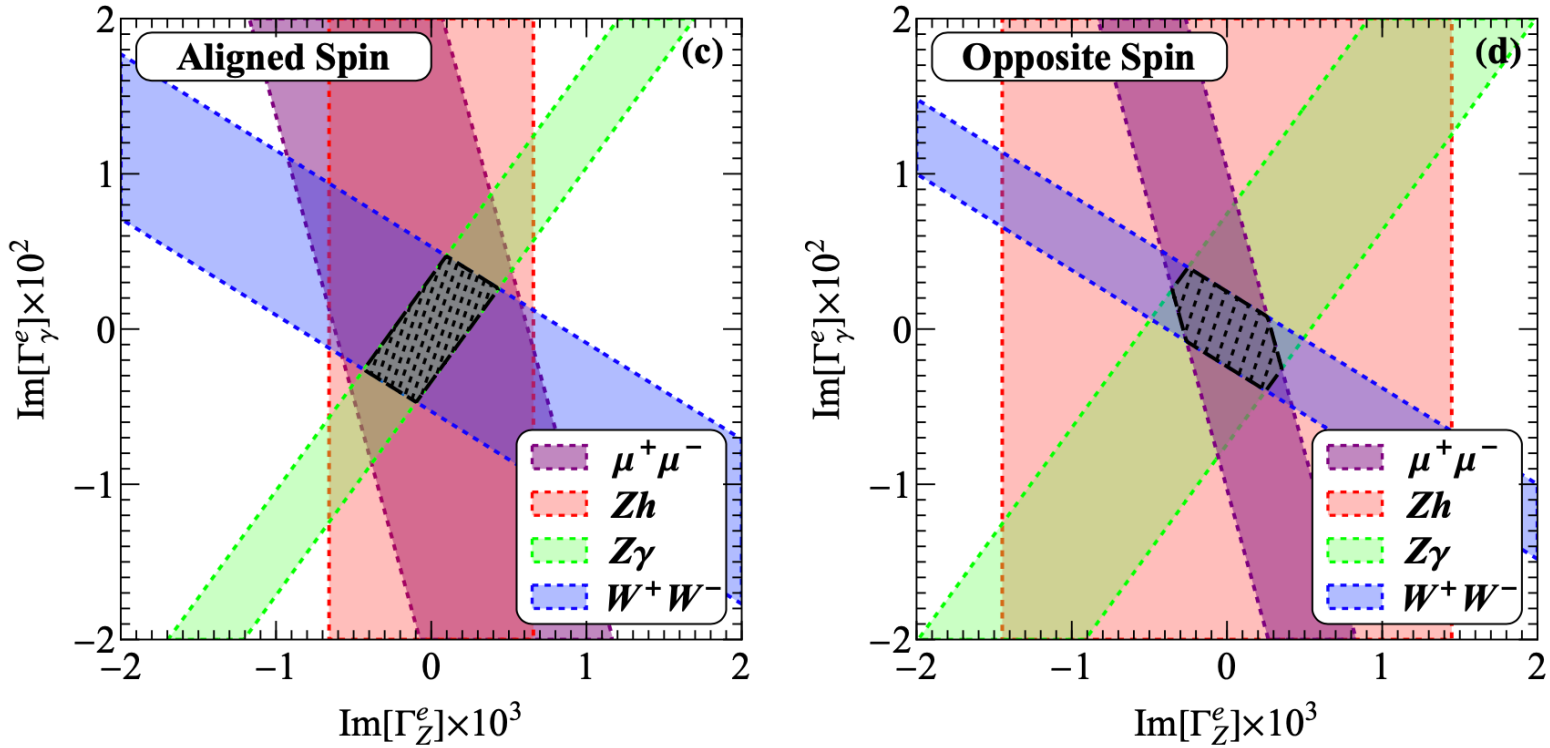

Offering a new opportunity for directly probing potential CP-violating effects.

Summary

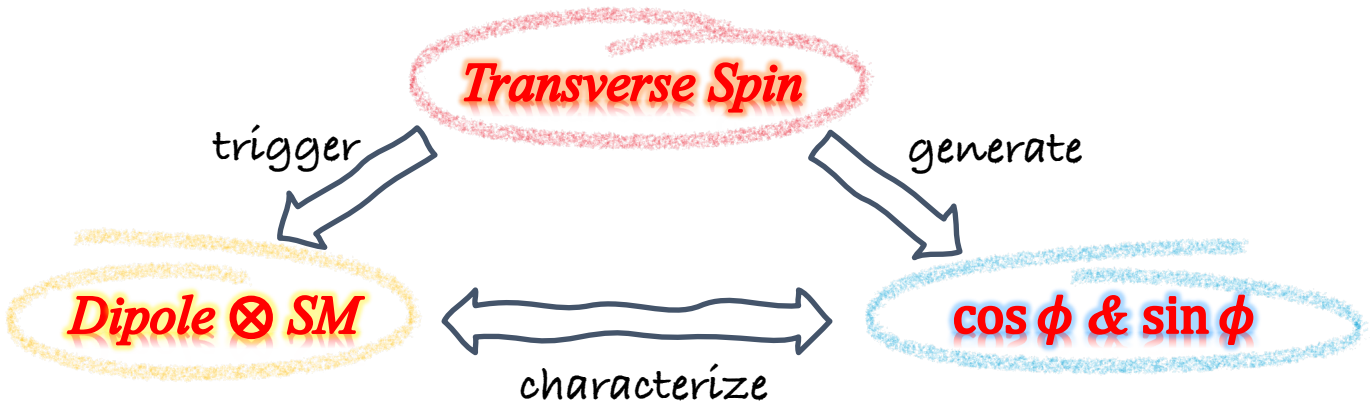

- ✓ Dipole operators flip fermion helicities being ideally studied at $1/\Lambda^2$ through--

Single Transverse Spin Azimuthal Asymmetries

- ✓ STSAA simultaneously determining both Re & Im parts *without impact from other NP*, offering a new opportunity for directly probing potential CP-violating effects.
- ✓ Our bound could be reached around O(0.01%~0.1%), much stronger sensitivity than other approaches by 1~2 orders of magnitude

	$\lvert\Gamma_Z^e\rvert$	$\lvert\Gamma_A^e\rvert$
Our Study	**0.0002**	**0.005**
LHC Drell-Yan	0.0765	0.197
Z Partial Width	0.0582	0.093
$(g-2)_e$	10^{-2}	10^{-6}

Thank you

Backup

BACKUP

Backup: Some Formulae

$$|\Theta,\chi\rangle_1 = \cos\frac{\Theta}{2}|h=+\rangle + \sin\frac{\Theta}{2}e^{i\chi}|h=-\rangle$$

Superposition of the two helicity states along polarization $\vec{s}(\Theta,\chi)$

$$T_{h\bar{h}} = \langle\phi,\ldots|T|\chi,\bar{\chi}\rangle = \langle\phi=0,\ldots|T|\chi-\phi,\bar{\chi}-\phi\rangle$$

2-to-2 rotational invariance

Ken-ichi Hikasa, *Phys.Rev.D* 33 (1986) 3203, *PhysRevD*.38 (1988) 1439

$$|\mathcal{M}|^2(\boldsymbol{s},\bar{\boldsymbol{s}},\theta,\phi) = \sum_{\alpha_1,\alpha_2,\alpha_1',\alpha_2'} \rho_{\alpha_1,\alpha_1'}(\boldsymbol{s})\,\bar{\rho}_{\alpha_2,\alpha_2'}(\bar{\boldsymbol{s}})\,\mathcal{M}_{\alpha_1,\alpha_2}(i\to f;\theta,\phi)\,\mathcal{M}^\dagger_{\alpha_1',\alpha_2'}(i\to f;\theta,\phi)$$

$$\boldsymbol{s} = (b_1,b_2,\lambda) = (b_{\mathrm{T}}\cos\phi_0, b_{\mathrm{T}}\sin\phi_0,\lambda)$$

$$\rho = \frac{1}{2}(1+\boldsymbol{\sigma}\cdot\boldsymbol{s})$$

$$\mathcal{M}_{\lambda_1,\lambda_2}(\theta,\phi) = e^{i(\lambda_1-\lambda_2)\phi}\mathcal{T}_{\lambda_1,\lambda_2}(\theta)$$

$$|M|^2 = |M|^2_{\mathrm{unpol}} - \frac{1}{2}\lambda_T\bar{\lambda}_T\mathrm{Re}[T^*_{++}T_{--}] - \frac{1}{2}\lambda_T\bar{\lambda}_T\mathrm{Re}[e^{-2i\phi}T^*_{+-}T_{-+}] + \frac{1}{2}\lambda_T\mathrm{Re}\left[e^{-i\phi}(T^*_{+-}T_{--}+T^*_{++}T_{-+})\right] - \frac{1}{2}\bar{\lambda}_T\mathrm{Re}\left[e^{-i\phi}(T^*_{+-}T_{++}+T^*_{--}T_{-+})\right]$$

$$|\mathcal{M}|^2_{TU} = \frac{1}{2}b_{\mathrm{T}}\mathrm{Re}\left[e^{i(\phi-\phi_0)}\left(\mathcal{T}_{++}\mathcal{T}^\dagger_{-+}+\mathcal{T}_{+-}\mathcal{T}^\dagger_{--}\right)\right]$$

$$T_{-\lambda_a,-\lambda_b,-\lambda_c,-\lambda_d}(\theta) = \eta\cdot(-1)^{\lambda-\mu}\cdot T_{\lambda_a,\lambda_b,\lambda_c,\lambda_d}(\theta)$$

$$\eta = \frac{\eta_c\eta_d}{\eta_a\eta_b}\cdot(-1)^{s_a+s_b-s_c-s_d}$$

Backup: Polarized beam realization

Transverse polarization is more natural

Sokolov-Ternov effect (92.4%, minutes-hours, 50GeV)

Laser-assistant

Spin-precession

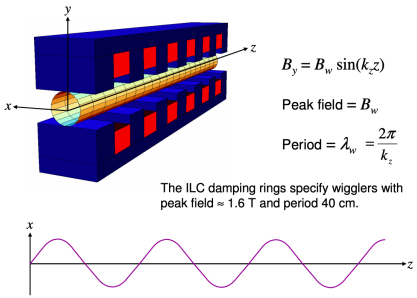

Photon-based scheme:

Polarized positrons are produced via pair production in a thin target from circularly-polarized photons with energy of multi-MeV (up to about 100 MeV). The cost difference between an polarized source and an upgrade from a unpolarized source is small (~ 1%). At 500 GeV, loss of polarization <1%, at IP <0.25%.

Polarized electron source consists of a polarized high-power laser beam and a high-voltage dc gun with a semiconductor photocathode.

Only polarization parallel or anti-parallel to the guide fields of the damping ring is preserved. Need to avoid spin-orbit coupling resonance depolarizing effects.

The spin rotator systems between the damping rings and the main linacs *permit the setting of arbitrary polarization vector orientations* at the IP.

Polarized-photons source:

I. a high-energy electron beam (>~ 150 GeV) passing through a short period, helical undulator. (E-166, SLAC)

II. Compton backscattering of laser light off a GeV energy-range electron beam. (KEK)

In both schemes a polarization of about |Pe+ | ≥ 90% is reported.

G. Moortgat-Pick et al. *Phys.Rept.* 460 (2008), hep-ph/0507011

Backup: anomalous magnetic moment

Muon

$$a_\mu^{\rm exp} = 116\,592\,061(41) \times 10^{-11} \qquad |d_\mu| < 1.5 \times 10^{-19}\ e\text{–cm} \qquad @\,90\%\,\text{CL}$$

$$a_\mu^{\rm SM} = 116\,591\,810(43) \times 10^{-11} \qquad \Delta a_\mu = a_\mu^{\rm exp} - a_\mu^{\rm SM} = 251(59) \times 10^{-11}$$

the spin vector's precession in the muon rest frame

the rate of spin precession relative to the muon momentum direction ~ MDM and EDM

$\vec{\omega}_a + \vec{\omega}_{\rm EDM}$, where, in the approximation $\vec{\beta} \cdot \vec{B} \approx 0$,

$$\vec{\omega}_a = -\frac{q}{m}\left[a_\mu \vec{B} + \left(-a_\mu + \frac{1}{\gamma^2 - 1}\right)\vec{\beta} \times \frac{\vec{E}}{c}\right]. \qquad (2)$$

In the approximation $\vec{\beta} \cdot \vec{E} \approx 0$,

$$\vec{\omega}_{\rm EDM} = -\eta \frac{q}{2m}\left(\vec{\beta} \times \vec{B} + \frac{\vec{E}}{c}\right) = -\frac{\eta}{2mc}\vec{F}, \qquad (3)$$

As noted above, a non-zero EDM increases the total spin precession frequency

$$\omega = \omega_a \sqrt{1 + \tan^2 \delta}. \qquad (16)$$

Muon (g-2) Collaboration, G.W. Bennett et al., *Phys.Rev.D* 80 (2009)

Backup: anomalous magnetic moment

Electron $a_e^{\rm exp} = 1\,159\,652\,180.73(28) \times 10^{-12}$ $\quad |d_e| < 1.1 \times 10^{-29}\ e\text{–cm}$ $\quad$ @ 90% CL

D. Hanneke et al., *Phys. Rev. Lett.* 100 (2008) 120801 ACME Collaboration, V. Andreev et al., *Nature* 562 (2018)

SM prediction crucially depends on the input value for the fine-structure constant

$$\alpha^{-1}_{\rm QED,Cs} = 137.035999046(27) \qquad a_e^{\rm SM,Cs} = 1\,159\,652\,181.61(23) \times 10^{-12}, \qquad \Delta a_e^{\rm Cs} = a_e^{\rm exp} - a_e^{\rm SM,Cs} = -0.88(36) \times 10^{-12},$$

$$\alpha^{-1}_{\rm QED,Rb} = 137.035999206(11) \qquad a_e^{\rm SM,Rb} = 1\,159\,652\,180.252(95) \times 10^{-12}, \qquad \Delta a_e^{\rm Rb} = a_e^{\rm exp} - a_e^{\rm SM,Rb} = 0.48(30) \times 10^{-12},$$

Fig. 3 represents the lowest cyclotron and spin energy levels for an electron weakly confined in a vertical magnetic field $B\hat{\mathbf{z}}$ and an electrostatic quadrupole potential. The latter is produced by biasing the trap electrodes of Fig. 2. The measured cyclotron frequency $\bar{f}_c \approx 149$ GHz (blue in Fig. 3) and the measured anomaly frequency $\bar{\nu}_a \approx 173$ MHz (red in Fig. 3) mostly determine $g/2$ [2]

$$\frac{g}{2} \simeq 1 + \frac{\bar{\nu}_a - \bar{\nu}_z^2/(2\bar{f}_c)}{\bar{f}_c + 3\delta/2 + \bar{\nu}_z^2/(2\bar{f}_c)} + \frac{\Delta g_{cav}}{2}, \qquad (2)$$

with only small adjustments for the measured axial frequency $\bar{\nu}_z \approx 200$ MHz, the relativistic shift $\delta/\nu_c \equiv h\nu_c/(mc^2) \approx 10^{-9}$, and the cavity shift $\Delta g_{cav}/2$. The latter is the fractional shift of the cyclotron frequency caused by the interaction with radiation modes of the trap cavity. The Brown-Gabrielse invariance theorem [9] has been used to eliminate the effect of both quadratic distortions to the electrostatic potential, and misalignments of the trap electrode axis with $\mathbf{B}$. Small terms of higher order in $\bar{\nu}_z/\bar{f}_c$ are neglected.

Quantum jump spectroscopy determines $\bar{f}_c$ and $\bar{\nu}_a$.

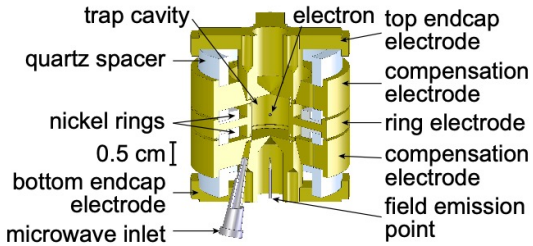

FIG. 2. Cylindrical Penning trap cavity used to confine a single electron and inhibit spontaneous emission.

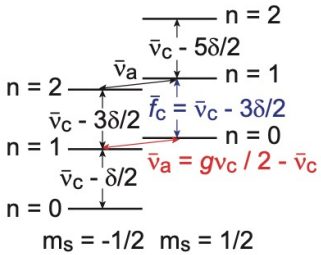

FIG. 3. Electron's lowest cyclotron and spin levels.

Backup: anomalous magnetic moment

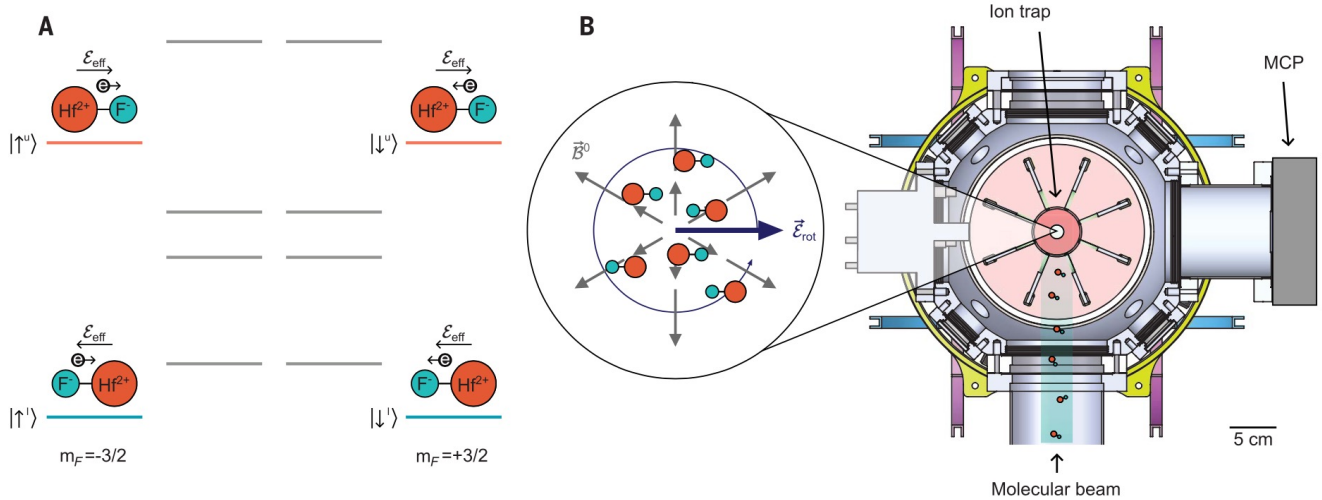

Fig. 1. Experiment outline. (**A**) Level structure of the eEDM-sensitive $^3\Delta_1$ ($v = 0, J = 1$) state. The horizontal axis indicates m_F, the projection of the total angular momentum onto the externally applied electric field. The vertical axis indicates the energy of the states. The direction of the electron spin and effective electric field, $\mathcal{E}_{\mathrm{eff}}$, is indicated for each of the states used in the experiment. (**B**) Schematic of ion trap, composed of eight radial electrodes and a pair of endcap electrodes. (Inset) Fields applied during experimental sequence: the rotating electric bias field, $\vec{\mathcal{E}}_{\mathrm{rot}}$, and the quadrupole magnetic field, $\vec{\mathcal{B}}^0$.

美国实验天体物理联合研究所（JILA）的研究团队将电子电偶极矩（eEDM）上界值压缩到4.1×10^{-30} e · cm，比之前的最好结果提升了2.4倍。该成果于2023年7月6日发表在《科学》杂志上。为了评估电子的形状，研究团队观察了电子在电场中的旋转情况。如果电子不是球形而是稍微偏向一侧（有电偶极矩，eEDM），电场将对其施加扭矩，就像重力使一个竖立的鸡蛋倾倒一样。与原子相比，使用分子可以提高对eEDM的测量精度。为了观察到这种扭矩，研究团队观察了铪氟化物分子（HfF+）的带电能级变化，对电子施加的扭矩将导致分子在相对于电场方向不同的取向下有不同的能级。他们探测了电子的磁矩与分子内电场同向与反向两种构型之间的能级位移，从而得到了eEDM大小的上界为4.1×10^{-30} e · cm 。

JILA Group, Tanya S. Roussy et al., *Science* 381,46-50(2023)

Backup: eEDM

$|d_e| < 1.1 \times 10^{-29}$ e–cm @ 90% CL

ACME Collaboration, V. Andreev et al., *Nature* 562 (2018)

目前全世界最精确的电子电偶极矩(electron Electric Dipole Moment, eEDM)上限的测量结果, $|de| < 1.1 \times 10^{-29}$e · cm (90% C. L.),是由第二代ACME 实验于2018年10月发布的。 ACME实验使用缓冲气体冷却的重极性分子ThO来测量电子电偶极矩. 在ThO分子处于电场中时,由于电子电偶极矩的存在会导致某些分子态能级会发生微小的移动。 ThO分子由脉冲激光轰击样品后经缓冲气体冷却 (Cryogenic buffer gas cooling) 从腔室内飞出形成分子束. 之后分子进入磁屏蔽 (Magnetic shielding) 区域,激光将分子制备到对电子电偶极矩最灵敏的 ‘H’态,然后被另一束泵浦光极化角动量.在此之后, 电子角动量在均匀的电场和磁场中进动, 进动角 (precession angle) 依赖于电子电偶极矩大小. 之后进动角被激光读出.电子电偶极矩可以由反转电场方向条件下的进动角之差得出。

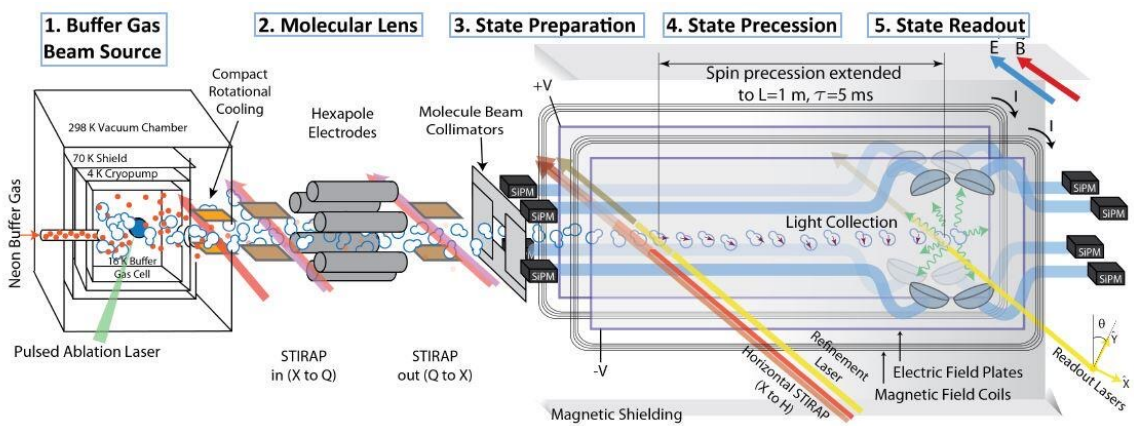

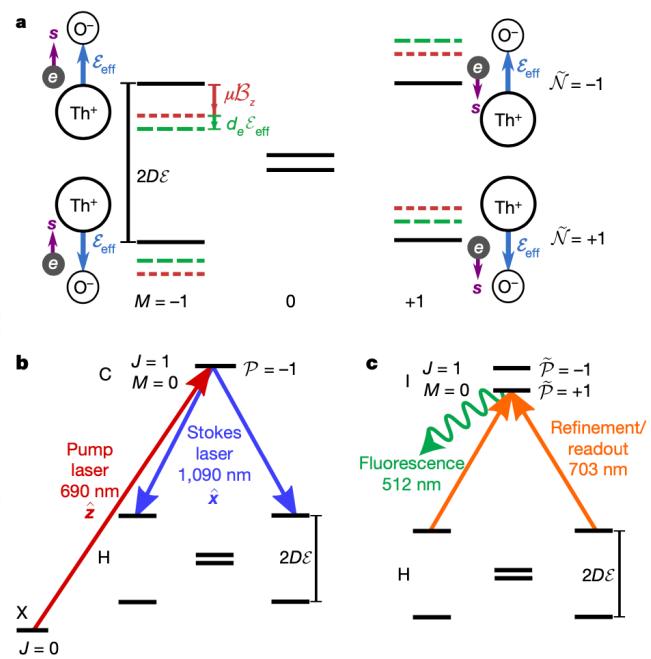

Backup: eEDM

$|d_e| < 1.1 \times 10^{-29}\ e\text{–cm}$ @ 90% CL

ACME Collaboration, V. Andreev et al., *Nature* 562 (2018)

•**极性分子.** 极性分子是目前已知对电子电偶极矩最敏感的系统.其分子内原子间电场可达几十吉伏/厘米 (gigavolts per centimeter, GV/cm), 几乎是实验室可制备电场强度大小的数百万倍. 由于电子电偶极矩的能量正比于其所在电场强度大小,分子的电子轨道上的电子会经历较强的电场并且产生相对较大的能级移动. 对于ThO分子计算表明该分子内原子间电场可达 84GV/cm,为目前已知分子之最.

•**分子原位磁强计.**某些情况下漏电磁场也会导致分子能级移动, 而被误认为是电子电偶极矩所引起的. 本实验中的分子的 ‘H’态能级结构中有奇偶能级对 (Parity Doublet).该能级对在零场时相差数百kHz, 因此可以被很小的外部电场极化, 而该能级对在电子电偶极矩影响下的能级移动大小相同, 方向相反. 选用能级对中不同能态相当于在不反转分子所在外场的方向时,反转分子内部电子所经历的内部电场方向.因此通过选取能级对中的不同能级, 我们可以反转分子内部电场并抵消许多由电磁场引起的系统性误差.

•**冷分子束.** 缓冲气体冷却的分子束的冷却效果受流体效应进一步增强,能形成低温慢速高流量的分子束流. 本实验中的ThO分子束在无需激光减速及Stark减速的条件下,能达到单位立体角内基态分子平均通量10^13 分子/秒及 170米/秒的平均速度.